Electrocatalytic Oxidation of Ethylene Glycol at Palladium-Bimetallic Nanocatalysts (PdSn and PdNi) Supported on Sulfonate-functionalised Multi-walled Carbon Nanotubes

Tendamudzimu Ramulifho[a,b], Kenneth I. Ozoemena[*,a,b], Remegia M. Modibedi[a,*], Charl J. Jafta[a] and Mkhulu K. Mathe[a]

[a.] *Energy and Processes Unit, Materials Science and Manufacturing, Council for Scientific & Industrial Research (CSIR), Pretoria 0001, South Africa.*

[b.] *Department of Chemistry, University of Pretoria, Pretoria 0002, South Africa.*

Revised manuscript: Ms. No.: JELECHEM-D-12-00802

[*]Corresponding authors: (K.I. Ozoemena): Tel.:+27128413664; Fax: +27128412135; E-mail: kozoemena@csir.co.za; (R.M. Modibedi): Tel.:+27128412516; E-mail: mmodibedi@csir.co.za

Abstract

Electrocatalytic oxidation of ethylene glycol (EG) in alkaline medium using nano-scaled palladium-based bimetallic catalysts (Pd-M, where M = Ni and Sn) supported on sulfonated multi-walled carbon nanotubes (SF-MWCNTs) is compared. The bimetallic mixture (i.e., SF-MWCNT-$PdSn_{mix}$ and SF-MWCNT-$PdNi_{mix}$) showed better electrocatalysis towards EG oxidation than the SF-MWCNT-Pd. At the SF-MWCNT-$PdSn_{mix}$ platform, oxidation of EG occurred at lower onset and peak potentials, higher current density, and faster kinetics (lower impedance) than at the SF-MWCNT-$PdNi_{mix}$ platform. EG oxidation at the SF-MWCNT-$PdNi_{mix}$ is more stable than at the SF-MWCNT-$PdSn_{mix}$. Indeed, Sn is a more favoured co-catalyst with Pd in EG electro-oxidation.

Keywords: Ethylene glycol; Electro-oxidation; Bimetallic catalysts; PdSn nanocatalyst.

1. Introduction

Direct alcohol alkaline fuel cells (DAAFCs) have continued to attract major research interests in the field of electrochemical energy conversion systems. DAAFCs are suitable fuel cell systems that employ a wide range of liquid fuels such as methanol, ethanol, glycerol and ethylene glycol (EG) due to their high specific energy and capacity of some of them to be renewable [1,2]. In the last couple of years, several reports have emerged on fuel cell systems that could potentially utilize EG as the liquid fuel using different electrocatalysts [3,4]. EG is a diol-alcohol that can be obtained from the bio-mass, it is non-toxic, has high reactivity and is a renewable fuel [5,6]. While the electro-oxidation of many other alcohols has been intensively studied in alkaline media [7-12], the electro-oxidation of EG in alkaline remains the least explored.

The use of the alkaline medium allows the use of platinum free electrocatalysts, eliminating the problem of the catalysts poisoning by carbon monoxide (CO) and improving the alcohol electro-oxidation kinetics [13]. Palladium is considered as a suitable electrocatalyst for alcohol oxidation in alkaline medium since it is more abundant in nature, less expensive than platinum and has the capacity to promote the oxidation of several alcohols in alkaline medium with remarkable electrochemical stability [2,7-14]. The catalyst support material also plays a great role on the catalyst performance. Carbon materials with high surface area and good crystallinity provide a high

dispersion of catalyst particles and facilitate electron transfer, resulting in better device performance. Studies [15–18] have shown that carbon nanotubes increase the electrocatalytic properties of several metal catalysts. Electro-oxidation of EG using platinum group metal electrocatalysts supported on CNTs has been explored in acid medium [19,20]. Surprisingly, however, despite the many advantages of EG as a fuel cell in alkaline media, the electro-oxidation of EG on Pd and Pd-based electrocatalysts in alkaline medium still remains hugely unexplored or reported in the literature. To our knowledge the only known work is that by Sun et al [23] where the authors used Pd nanoparticles supported on sulfonate-functionalised multi-walled carbon nanotubes (SF-MWCNTs). Recently, it was shown that Pd bimetallic catalysts on SF-MWCNTs exhibit better performance towards ethanol electro-oxidation compared to monodispersed Pd nanoparticles [22,24]. Thus, motivated by the paucity of literature on EG electro-oxidation on Pd alloy catalysts in alkaline media, and the poor performance of monodispersed Pd nanocatalysts compared to the Pd bimetallic catalysts, we decided to investigate the electrocatalytic behavior of the Pd bimetallic catalysts (SF-MWCNT-PdNi and SF-MWCNT-PdSn) towards the oxidation of EG in alkaline medium. We clearly show (using voltammetric and electrochemical impedance spectroscopic techniques) that these Pd bimetallic nanocatalysts serve as efficient electrocatalysts for the oxidation of EG in alkaline medium, albeit slight differences in their individual catalytic behaviour.

2. Experimental

2.1 Materials and reagents

Absolute ethanol (C_2H_5OH, ACS reagent grade), multi-walled carbon nanotubes (≥ 95% as MWCNT, O.D × I.D × length, 7-15 nm × 3-6 nm × 0.5 – 200 μm), hydrogen peroxide (H_2O_2, 30 % by weight), Nafion perfluorinated ion-exchange resin (5 wt% in mixture of lower aliphatic alcohols), potassium hydroxide pellets (KOH, ACS reagent, > 85% pure), Sulfuric acid (H_2SO_4, 95 – 97 % pure), tin (II) chloride dehydrate ($SnCl_2$. $2H_2O$, 99.995%) were obtained from Sigma-Aldrich. Acetic anhydride ($(CH_3\text{-}CO)_2O$, ACS reagent grade), ethylene glycol ($OHCH_2CH_2OH$, extra pure), and nitric acid (HNO_3, 65% extra pure) were obtained from Merck. Hydrophilic polypropylene membrane filters, 47 mm in diameter and 0.2 μm pore size were obtained from Pall Corporation. Nickel chloride ($NiCl_2$, 60 mesh 99.5% pure) was obtained from Cerac Incorporated. Palladium (II) chloride ($PdCl_2$) was obtained from SA Precious Metal (Pty) Ltd (South Africa). Ultrapure water (resistivity: 18.2 MΩcm) was obtained from a Milli-Q water system (Millipore Corp., Bedford, MA, USA). All other reagents were of analytical grade and were used as received from the suppliers without further purification.

2.2 Catalysts synthesis

2.2.1 Sulfonation of multi-walled carbon nanotubes

The pristine MWCNTs were functionalised with sulfonate groups following the method described by Sun *et al*. [23]. After the initial treatment of purification and carboxylate-functionalisation of the pristine MWCNTs [25], the solid product was then sulfonated. 120 mg of the previously purified MWCNTs was added to a mixture of 20 mL H_2SO_4 and 300 mL of acetic anhydride, holding continuous stirring at 70 °C for 2 h. After 2 h, the reaction mixture was allowed to cool, continuously stirred until room temperature. The resulting product (abbreviated herein as SF-MWCNT) was repeatedly washed with ultra pure water and dried at 70 °C overnight in an oven.

2.2.2 Preparation of the bimetallic PdM (M = Ni, Sn) supported on SF-MWCNTs and electrode modification

The metal (Pd, Ni and Sn) nanoparticle catalysts were supported onto the walls of the SF-MWCNTs by adopting the microwave polyol process as reported in the literature [26]. In brief, 3.0 mL of 0.05 M aqueous $PdCl_2$ solution and 50 mL of EG were introduced into a 250 ml Erlenmeyer flask. The synthesis solution pH was adjusted to ~ 7.4 by using 0.8 M aqueous KOH solution. 80 mg of SF-MWCNTs was then added into the above solution and ultrasonically dispersed in the solution for 1 h. The solution was then transferred into a liner-rotor 16 F100 TFM vessel, then placed in a microwave

(Multiwave 3000 sample preparation system, 1400 Watts, Anton Paar) and heated using 1000 Watts at 170 °C for 60 s. The time taken to reach 170 °C was 13 min, and then the microwave was stopped, allowed to cool before the reaction vessel could be removed. The resulting suspension was separated by filtration and the obtained residue washed with acetone and ultra pure water. The final solid product (abbreviated herein as SF-MWCNT-Pd) was dried at 110 °C overnight in an oven. The SF-MWCNT-Sn and SF-MWCNT-Ni were prepared using a similar procedure to the SF-MWCNT-Pd using $SnCl_2$ and $NiCl_2$ precursors (i.e., 3.0 mL of 0.05 M aqueous $NiCl_2$ or $SnCl_2$ solution in 50 mL of EG used in the microwave reaction). The ratios of Pd, Sn or Ni were controlled by stoichiometric calculation and confirmed by energy dispersive X-ray spectroscopy (EDX) measurements.

To prepare the bimetallic catalysts (SF-MWCNT-PdM_{mix}), 2 mg mixture of SF-MWCNT-Pd and SF-MWCNT-Ni or SF-MWCNT-Sn was thoroughly dispersed in 2 ml ethanol and 100 μL 5wt % Nafion® solution with the aid of ultrasonic stirring (Bransonic 52 bath, operating frequency of ~ 40 KHz). To allow for proper mixing and interaction of the bimetals, each mixture was ultrasonicated in a tightly closed container for 4 h at 40 ^{o}C, and then allowed to stay for ~ 24 h before drying. The bimetallic catalysts formed are abbreviated as GCE-SF-MWCNT-$PdNi_{mix}$ and GCE-SF-MWCNT-$PdSn_{mix}$. To immobilize them on the glassy carbon electrode (GCE), the GCE was first polished to a mirror finish with alumina slurry (nanopowder, Aldrich) and

then cleaned by ultrasonic stirring in acetone and deionised water for 3 min respectively. 10 μL of the mixture (pre-sonicated again for about 1 min) was then cast onto the surface of the cleaned GCE. The electrode was then dried at 80 °C in an oven. The Pd loading of each electrode was maintained at 6.7 μg.

2.3 Equipment and Procedures

The transmission electron microscope (TEM) micrographs were obtained using a JEOL 2010 TEM system operating at 200 kV. The TEM samples were prepared by dispersing the carbon supported catalysts in ethanol, and then a drop of the suspension was cast onto the carbon film covered Cu-grid for analysis. The X-ray diffraction (XRD) patterns of the catalysts were obtained using an X-ray diffractometer (XRD, SCINTAG-XDS 2000) with Cu Kα radiation source, λ=1.5418 Å operating at 40 kV and 200 mA. The XRD diffractograms were obtained in a scan range between 0 and 90°. Fourier-transform infrared (FTIR) spectra were recorded using Spectrum 100 FTRI spectrometer (Perkin Elmer). The energy dispersive x-ray spectra (EDX) were obtained from NORAN VANTAGE (USA). X-ray photoelectron spectroscopy (XPS) experiments were carried out on a Kratos Axis Ultra-DLD system (Shimadzu) with Mg Kα radiation (hυ = 1253.6 eV). Binding energies were calibrated using the signal of contamination carbon as reference (C1s = 284.6). The detailed XP spectra were collected and analysed at a 45° take-off angle (ϕ). All electrochemical experiments were carried out at room temperature

with a standard three-compartment electrochemical cell using an Autolab potentiostat PGSTAT 302 (Eco Chemie, Utrecht, Netherlands) driven by the General Purpose Electrochemical Systems data processing software (GPES and FRA softwares version 4.9). The working electrode was a modified glassy carbon disk electrode (GCE, Bioanalytical systems, diameter = 3.0 mm). A Pt rod and Ag|AgCl, saturated 3M KCl) were used as a counter and reference electrode, respectively. Electrochemical impedance spectroscopy (EIS) measurements were obtained with Autolab Frequency Response Analyser (FRA) software between 100 kHz and 10 mHz with the amplitude (rms value) of the AC signal of 10 mV. All solutions were de-aerated by bubbling pure nitrogen prior to each electrochemical experiment.

3. Results and discussion

3.1 XPS characterisation

As shown recently, the bimetallic catalyst obtained by ultrasonication of the monometallic mixtures (SF-MWCNT-PdNi$_{mix}$ and SF-MWCNT-PdSn$_{mix}$) showed enhanced electrocatalysis towards alcohol than that by co-reduction of the metals [22,24]. In this work, we use XPS as a further proof for the formation of alloy. Figure 1 compares the XPS patterns of the standard samples (i.e., SF-MWCNT-PdNi and SF-MWCNT-PdSn obtained by the conventional co-reduction of the metals, Sn and Ni) and the SF-MWCNT-PdNi$_{mix}$ and SF-MWCNT-PdSn$_{mix}$ (i.e., obtained by simple ultrasonication of

the metallic mixtures) showing the signature doublet consisting of a high-energy peak (Pd $3d_{3/2}$) and a low-energy peak (Pd $3d_{5/2}$), with a spin–orbit splitting of about 5 eV. The comparative XPS data are shown in Table 1.

Table 1: Comparison of the SF-MWCNTs supported PdM (M = Ni, Sn) alloys prepared by the standard co-reduction method and ultrasonication of the mixtures of metals.

Standard alloy on SF-MWCNTs				**'Mix' alloy on SF-MWCNTs**			
PdSn		**PdNi**		**$PdSn_{mix}$**		**$PdNi_{mix}$**	
Pd	**Sn**	**Pd**	**Ni**	**Pd**	**Sn**	**Pd**	**Ni**
335.6	485.4	335.3	-	335.3	485.5	335.4	-
336.4	487.0	336.5	-	336.4	487.0	336.6	-
337.9	-	337.8	-	337.9	487.6	338.2	-
338.7	-	-	-	-	-	-	-

The Pd $3d_{5/2}$ (alloy) peak gives four contributions which relate to the chemical states: 335.6±0.1 eV (PdSn), 336.4±0.1 eV (Pd_xO_y), 337.9±0.1 (Pd_xO_y) and 338.7±0.1 eV ($PdSO_4$). Interestingly, the Pd $3d_{5/2}$ (mix) peak gives similar contributions at 335.3±0.1 eV (PdSn), 336.4±0.1 eV (Pd_xO_y) and 337.9±0.1 eV (Pd_xO_y). Clearly, the surface chemistry of the $PdSn_{Alloy}$ and $PdSn_{Mix}$ are similar. As seen in Table 1, the same trend of peak evolutions and chemical compounds are observed for both PdNi (alloy) and PdNi (mix). The Pd $3d_{5/2}$ peak of our SF-MWCNT-$PdNi_{mix}$ (335.3 eV) is comparable to the binding

energy value (335.4 eV) recently reported for PdNi alloy supported on MWCNT [27], confirming that ultrasonic-mixing technique formed an alloy.

3.2 Electrochemical characterisation

3.2.1 Electro-oxidation of ethylene glycol in alkaline medium

Figure 2 shows the voltammetric responses of SF-MWCNT-Pd, SF-MWCNT-$PdNi_{mix}$ and SF-MWCNT-$PdSn_{mix}$ electrocatalysts towards ethylene glycol (EG) oxidation in 0.5 M KOH. The EG activity on the SF-MWCNT-$PdSn_{mix}$ catalyst is higher than that of the SF-MWCNT-$PdNi_{mix}$ and SF-MWCNT-Pd. The electrochemical parameters are summarized in Table 2. The beneficial effect of the Ni and Sn on the Pd systems for EG oxidation in alkaline medium may be related to the oxophilicity of the Ni and Sn to generate the M-OH moieties as speculated by Bambagioni *et al*. [28]. The SF-MWCNT-$PdSn_{mix}$ has the most negative onset potential, the highest current density and less positive peak potential as compared to the SF-MWCNT-$PdNi_{mix}$ catalyst. The ratio of the forward to the backward current (I_f/I_b) is highest for the SF-MWCNT-$PdSn_{mix}$, indicating better oxidation of the EG and that this catalyst mixture is less likely to be poisoned by the oxidation products compared to the SF-MWCNT-Pd and SF-MWCNT-$PdNi_{mix}$. The ratio of the current response of the forward anodic peak (I_f) to the reverse anodic peak (I_b) is a measure of the fraction of the catalyst surface that has not been poisoned; the higher the value of I_f/I_b, the less poisoned is the electrode. Within the error limits, the

value of I_f/I_b obtained for the SF-MWCNT-Pd (1.82) is comparable to the 1.94 observed by Sun *et al* [23]. The higher current response of the SF-MWCNT-$PdSn_{mix}$ electrode was further confirmed by performing chronoamperometric experiment at fixed potential of -0.2 V (not shown). The current value obtained for the SF-MWCNT-$PdSn_{mix}$ electrocatalyst was higher (11.59 mA cm^{-2}) than that obtained for SF-MWCNT-$PdNi_{mix}$ (9.75 mA cm^{-2}) and SF-MWCNT-Pd (6.91 mA cm^{-2}) electrocatalysts.

Table 2: Comparison of the electrochemical performances of ethanol oxidation on GCE-SF-MWCNT-Pd, GCE-SF-MWCNT-$PdSn_{mix}$ and GCE-SF-MWCNT-$PdNi_{mix}$ nanocomposites measured in a 0.5 M Ethylene glycol + 0.5 M KOH solution at a sweep rate of 50 mVs^{-1} (n = 9).

Electrocatalyst	Electrocatalytic performance data			
	J_f / $mAcm^{-2}$	E_{onset} / V	E_p / V	I_f/I_b
SF-MWCNT-Pd	19.1±0.02	-0.24±0.02	0.15±0.02	1.82
SF-MWCNT-$PdNi_{mix}$	35.3±0.02	-0.39±0.02	0.25±0.02	1.57
SF-MWCNT-$PdSn_{mix}$	51.9±0.02	-0.44±0.02	0.23±0.02	2.10

Figure 2b is a comparative quasi-steady state linear sweep voltammetric curves for EG oxidation on SF-MWCNT-Pd, SF-MWCNT-$PdNi_{mix}$ and SF-MWCNT-$PdSn_{mix}$ at 1 mV S^{-1}. As expected from previous

experiments, the SF-MWCNT-$PdSn_{mix}$ electrocatalyst shows the highest anodic current density compared to the SF-MWCNT-$PdNi_{mix}$ and SF-MWCNT-Pd electrocatalysts. The electrochemically-active surface areas (EASA) of the electrodes were determined in 0.5 M KOH and found to be 63.58 m^2g^{-1} for the SF-MWCNT-$PdSn_{mix}$, 58.82 m^2g^{-1} for the SF-MWCNT-$PdNi_{mix}$ and 60.44 m^2g^{-1} for the SF-MWCNT-Pd, indicating that Sn exerts more influence on the EASA of the Pd, and hence the high electrocatalytic activity.

3.2.2 Stability of electrocatalysts

Long-term chronoamperometry is constantly used to test the stability of electrocatalysts [29,30]. Thus, the stability of the SF-MWCNT-Pd, SF-MWCNT-$PdNi_{mix}$ and SF-MWCNT-$PdSn_{mix}$ were evaluated using chronoamperometric test. Figure 3 shows the chronoamperometric curves of the three catalysts in 0.5 M Ethylene Glycol in 0.5 M KOH solutions at a fixed potential of –0.2 V. In the first few seconds, the electrocatalysts showed small current decay with the SF-MWCNT-$PdSn_{mix}$ electrocatalyst showing higher current response (11.59 mA cm^{-2}) than that obtained for SF-MWCNT-$PdNi_{mix}$ (9.75 mA cm^{-2}) and SF-MWCNT-Pd (6.91 mA cm^{-2}). The current value of the SF-MWCNT-$PdSn_{mix}$ electrocatalyst remained higher throughout indicating higher stability of the SF-MWCNT-$PdNi_{mix}$ electrocatalyst. Values of the apparent current density for EG after 1200 s were 9.94, 8.13 and 4.67 $mAcm^{-2}$

respectively on SF-MWCNT-$PdSn_{mix}$, SF-MWCNT-$PdNi_{mix}$ and SF-MWCNT-Pd electrocatalyst. This indicates that SF-MWCNT-$PdSn_{mix}$ electrocatalyst is the more stable and more tolerant to poisoning compared to SF-MWCNT-$PdNi_{mix}$ and SF-MWCNT-Pd electrocatalysts in alkaline medium. Also, the SF-MWCNT-$PdSn_{mix}$ and SF-MWCNT-$PdNi_{mix}$ exhibited comparable CV behaviour as there was no detectable difference in the oxidation of EG in the presence or absence of carbon monoxide.

3.2.3 Electrochemical impedance analysis

The electrochemical kinetics of the three electrodes were further investigated using the electrochemical impedance spectroscopy in 0.5 M ethylene glycol + 0.5 M KOH at three different bias (0.2, 0.3 and 0.4 V vs Ag|AgCl sat'd KCl) (**Figure 4**). The impedance spectra were satisfactorily fitted with the $R_s(R_{ct}CPE)$ circuit, where R_s is the electrolyte resistance, R_{ct} is the charge transfer resistance and *CPE* is the constant phase element. The impedimetric data are summarised in Table 3. The R_{ct} is related to the reaction kinetics; its values of the SF-MWCNT-Pd and SF-MWCNT-$PdSn_{mix}$ electrodes decreased as the potential was increased from low to higher potentials (0.2 to 0.4 V), indicating faster electrode kinetics at higher potentials for EG oxidation. Generally, the SF-MWCNT-$PdSn_{mix}$ showed the least R_{ct} values compared to the two other electrodes.

Table 3: Impedimetric data for ethylene oxidation on GCE-SF-MWCNT-Pd, GCE-SF-MWCNT-$PdSn_{mix}$ and GCE-SF-MWCNT-$PdNi_{mix}$ nanocomposites measured in a 0.5 M ethylene glycol + 0.5 M KOH solution at different potentials

Bias / V	Electrochemical impedimetric parameter			
	R_s / Ω	R_{ct} / kΩ	n	10^2 CPE/ F
GCE-SF-MWCNT-Pd				
0.2	112.30±1.97	3.84 ±0.26	0.85±0.02	0.10±0.01
0.3	112.00±1.55	2.02 ±0.09	0.85±0.02	0.11±0.01
0.4	112.00 ±1.65	0.48 ±0.02	0.87±0.03	0.10±0.01
GCE-SF-MWCNT-$PdNi_{mix}$				
0.2	100.20±1.76	2.49 ±0.29	0.63±0.02	0.20 ±0.01
0.3	101.50±1.87	2.90±0.36	0.67±0.02	0.18 ±0.01
0.4	98.80±1.89	0.80±0.06	0.63±0.03	0.18 ±0.01
GCE-SF-MWCNT-$PdSn_{mix}$				
0.2	92.00±1.48	2.64 ±0.16	0.86 ±0.02	0.140 ±0.004
0.3	78.60 ±0.90	1.02 ±0.03	0.88 ±0.01	0.150 ±0.004
0.4	80.00 ±0.90	0.21 ±0.01	0.87 ±0.03	0.010 ±0.04

4. Conclusions

The electrocatalytic oxidation of ethylene glycol (EG) in alkaline medium has been investigated at Pd-based nano-scaled bimetallic alloy catalyst mixtures (PdSn and PdNi) supported on sulfonated multi-walled carbon nanotubes (SF-MWCNTs). XPS confirmed the properties of these alloy catalysts that were obtained by a simple ultrasonication. In terms of their electrocatalytic

properties, we observed very significant findings that should be emphasised. First, the bimetallic nanocomposite mixtures (SF-MWCNT-PdSn$_{mix}$ and SF-MWCNT-PdNi$_{mix}$) exhibited enhanced electrocatalytic EG oxidation compared to the Pd alone (i.e., SF-MWCNT-Pd). Second, the SF-MWCNT-PdSn$_{mix}$ electrode showed better electrocatalysis towards EG oxidation (in terms of low onset and peak potentials, high current density, and fast kinetics or low impedance) compared to the SF-MWCNT-PdNi$_{mix}$ platform. Third, from chronopotentiometric analysis, EG oxidation at the SF-MWCNT-PdNi$_{mix}$ is more stable than at the SF-MWCNT-PdSn$_{mix}$. Clearly, the two bimetallic alloy nanocatalysts showed some significant differences in their oxidation of EG. It does seem, however, that Sn may be a more favoured co-catalyst with Pd for possible application in direct ethylene glycol alkaline fuel cell technology.

Acknowledgements

We thank the CSIR and NRF for supporting this work. T. Ramulifho thanks the CSIR for MSc studentship at the University of Pretoria.

References

[1] H. Yue, Y. Zhao, X. Ma, J. Gong, Chem. Soc. Rev. 41 (2012) 4218–4244.

[2] V. Bambagioni, C. Bianchini, A. Marchionni, J. Filippi, F. Vizza, J. Teddy, P. Serp, M. Zhiani, J. Power Sources 190 (2009) 241-251.

[3] A. Serov, C. Kwak, Applied Catalysis B: Environmental 97 (2010) 1-12.

[4] K. Matsuoka, Y. Iriyama, T. Abe, M. Matsuoka, Z. Ogumi, J. Power Sources 150 (2005) 27-31.

[5] M.S. Ureta-Zañartu, C. Yáñez, M. Páez, G. Reyes, J. Electroanal. Chem. 405 (1996) 159-167.

[6] A.A. El-Shafei, S.A.A. El-Maksoud, A.S. Fouda, J. Electroanal. Chem. 395 (1995) 181-187.

[7] Z. Yan, G. He, G. Zhang, H. Meng, PK. Shen, Int. J. Hydrogen Energy 35 (2010) 3263-3269.

[8] Y. Zhao, L. Zhan, J. Tian, S. Nie, Z. Ning, Int. J. Hydrogen Energy 35 (2010) 10522 -10526.

[9] RM. Modibedi, T. Masombuka, MK. Mathe, Int. J. Hydrogen Energy 36 (2011) 4664-4672.

[10] X. Wang, W. Wang, Z. Qi, C. Zhao, H. Ji, Z. Zhang, Electrochem. Commun. 11 (2009) 1896–1899.

[11] AO. Neto, MM. Tusi, NS. de Oliveira Polanco, SG. da Silva, MC. dos Santos, EV. Spinace, Int. J. Hydrogen Energy,36 (2011) 10522-10526.

[12] R. Kazemi, A. Kiani, Int. J. Hydrogen Energy 37 (2012) 4098-4106.

[13] C. Coutanceau, L. Demarconnay, C. Lamy, J.-. Léger, J. Power Sources 156 (2006) 14-19.

[14] Q. Yi, F. Niu, L. Song, X. Liu, H. Nie, Electroanalysis 23 (2011) 2232 – 2240

[15] H.T. Zheng, Y. Li, S. Chen, P.K. Shen, J. Power Sources 163 (2006)371-375.

[16] S. Iijima, Physica B: Condensed Matter 323 (2002) 1-5.

[17] C.E. Banks, R.G. Compton, Analyst 131 (2006)15-21.

[18] J.H. Zagal, S. Griveau, K.I. Ozoemena, T. Nyokong and F. Bedioui, J. Nanosci. Nanotechnol. 9 (2009) 2201-2214.

[19] N.W. Maxakato, K.I. Ozoemena, C.J. Arendse, Electroanalysis 22 (2010) 519-529.

[20] N.W. Maxakato, C.J. Arendse K.I. Ozoemena, Electrochem. Commun. 11 (2009) 534-537.

[21] J.M. Sieben, M.M.E. Duarte, Int. J. Hydrogen Energy 36 (2011) 3313-3320.

[22] T. Ramulifho, MSc thesis (2010), University of Pretoria.

[23] Z. Sun, X. Zhang, Y. Liang, H. Li, J. Power Sources 191 (2009) 366-370.

[24] T. Ramulifho, K.I. Ozoemena, R.M. Modibedi, C.J. Jafta, M.K. Mathe, Electrochim. Acta 59 (2012)310-320.

[25] M.P. Siswana, K.I. Ozoemena, T. Nyokong, Electrochim. Acta 52 (2006) 114-122.

[26] X. Li, W. Chen, J. Zhao, W. Xing, Z. Xu, Carbon, 43 (2005) 2168-2174.

[27] R. Li, Z. Wei, T. Huang, A. Yu, Electrochim. Acta 56 (2011) 6860.

[28] V. Bambagioni, M. Bevilacqua, C. Bianchini, J. Filippi, A. Marchionni, F. Vizza, L.Q. Wang, P.K. Shen, Fuel Cells 10 (2010) 582-590.

[29] Y. Zhao, L. Zhan, J. Tian, S. Nie, Z. Ning, Int. J. Hydrogen Energy 35 (2010) 10522 -10526.

[30] Z. Qi, H.Geng, X.G.Wang, C.C.Zhao, H. Ji, C. Zhang,J.L.Xu, Z.G.Zhang, Journal of Power Sources 196 (2011) 5823–5828 J. Power Sources 196 (2011) 5823-5828.

LIST OF FIGURES

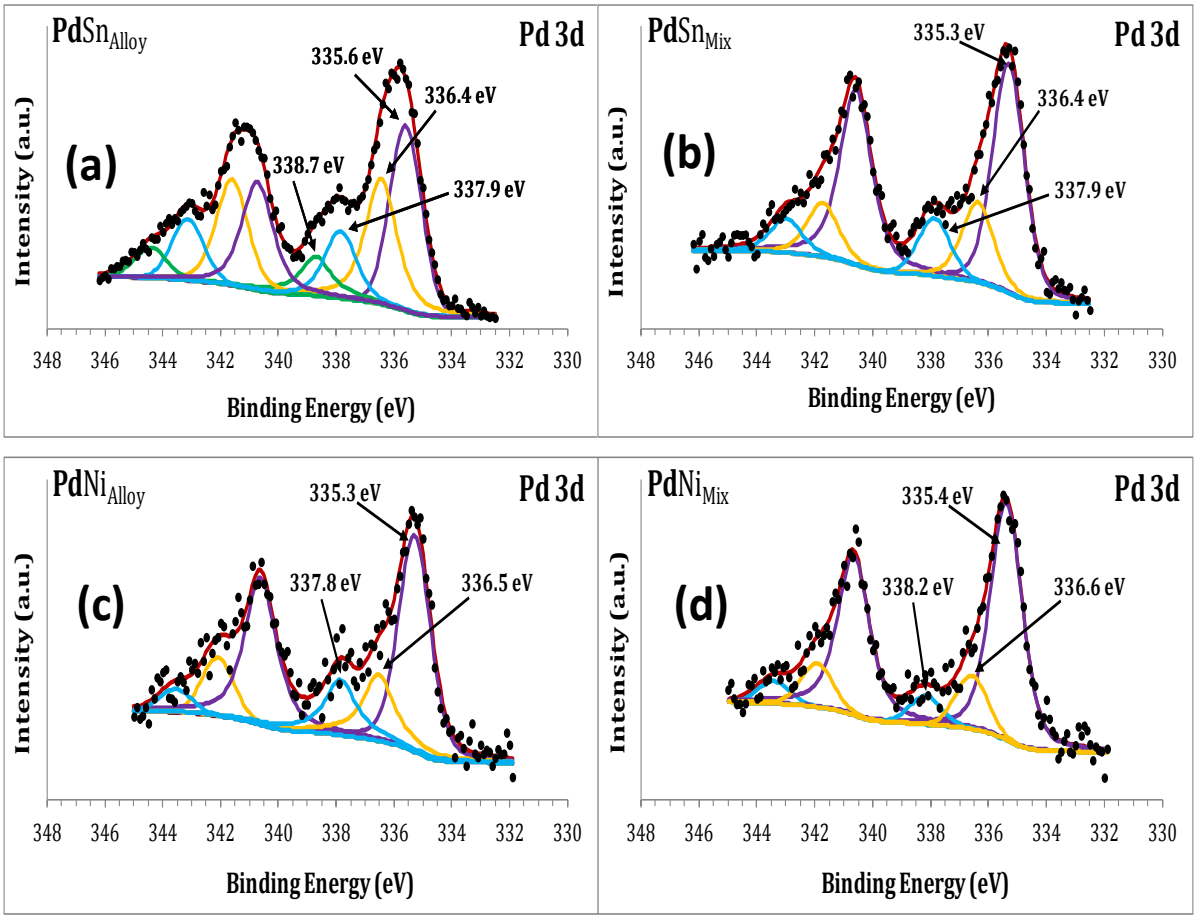

Figure 1: Typical XPS evolutions of Pd 3d of (a) $PdSn_{alloy}$ and (b) $PdSn_{mix}$, and (c) $PdNi_{alloy}$ and (d) $PdNi_{mix}$.

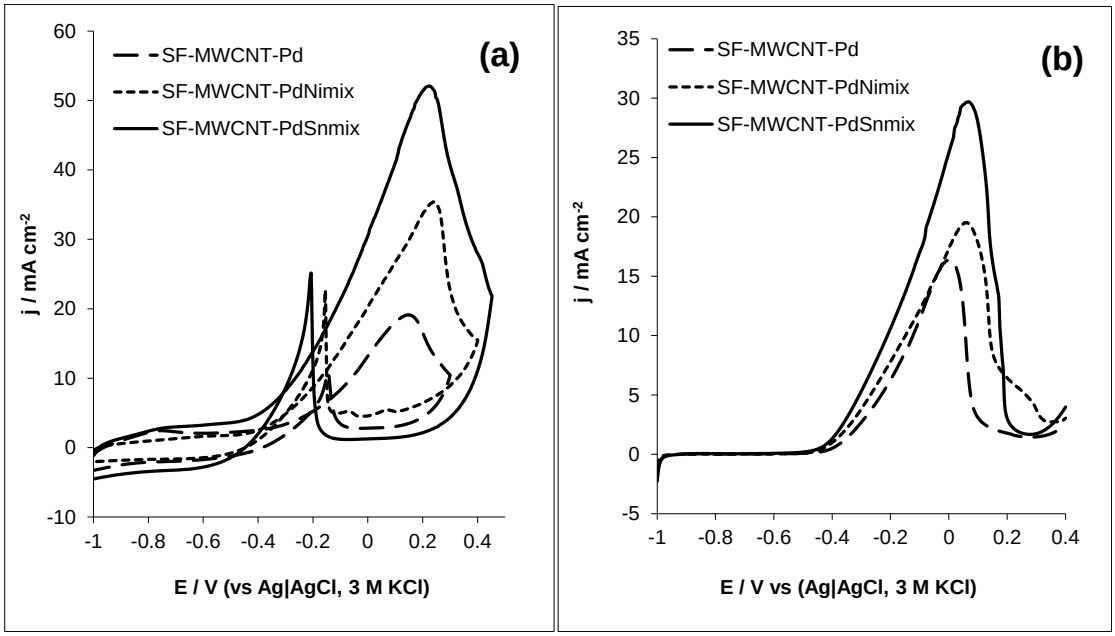

Figure 2: (a) Cyclic voltammograms at 50 mVs^{-1} and (b) quasi-steady state linear sweep voltammograms at 1 mVs^{-1} of SF-MWCNT-Pd, SF-MWCNT-$PdNi_{mix}$ and SF-MWCNT-$PdSn_{mix}$ in 0.5 M Ethylene glycol + 0.5 M KOH aqueous solutions.

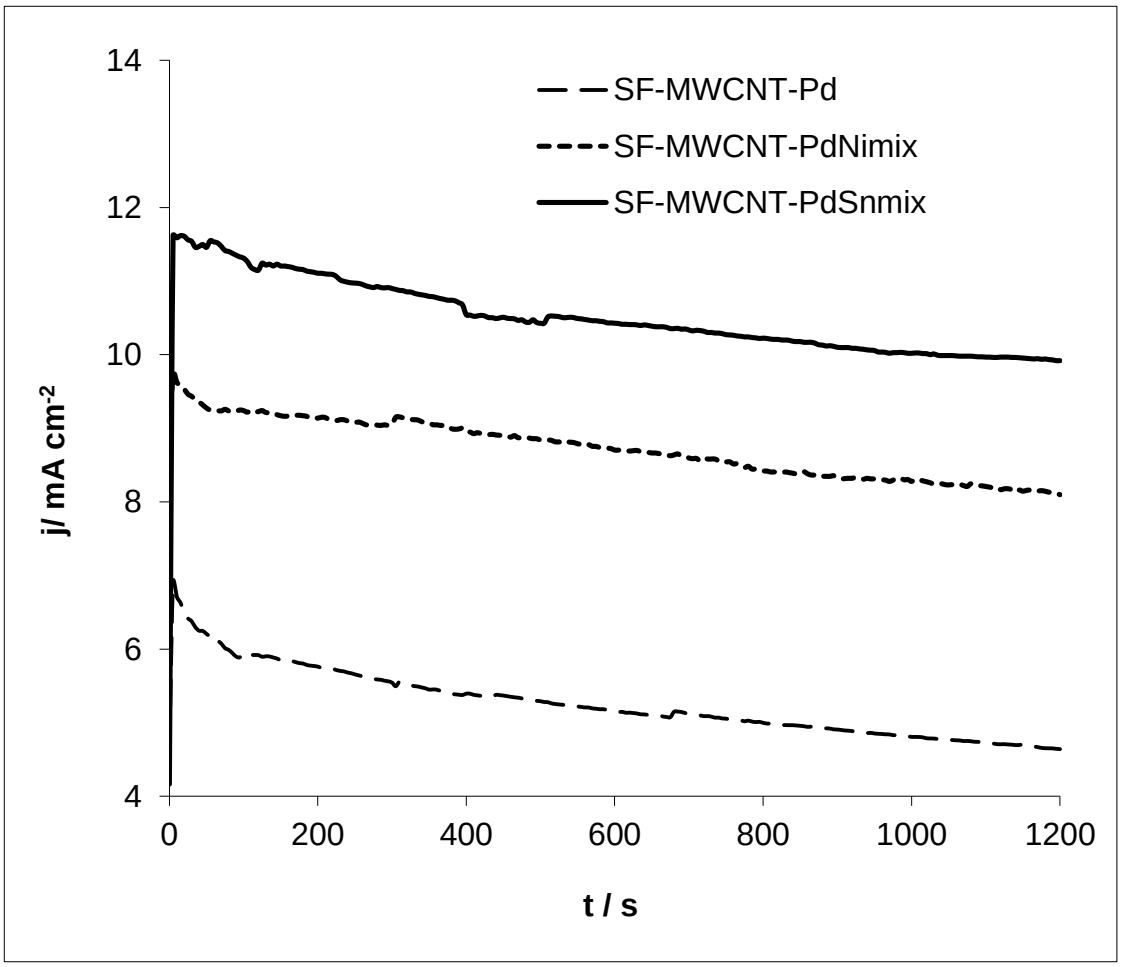

Figure 3: Chronoamperometric curves of GCE-SF-MWCNT-Pd, GCE-SF-MWCNT-$PdSn_{mix}$ and GCE-SF-MWCNT-$PdNi_{mix}$ in 0.5 M EG + 0.5 M KOH aqueous solutions at fixed potential of –0.2 V.

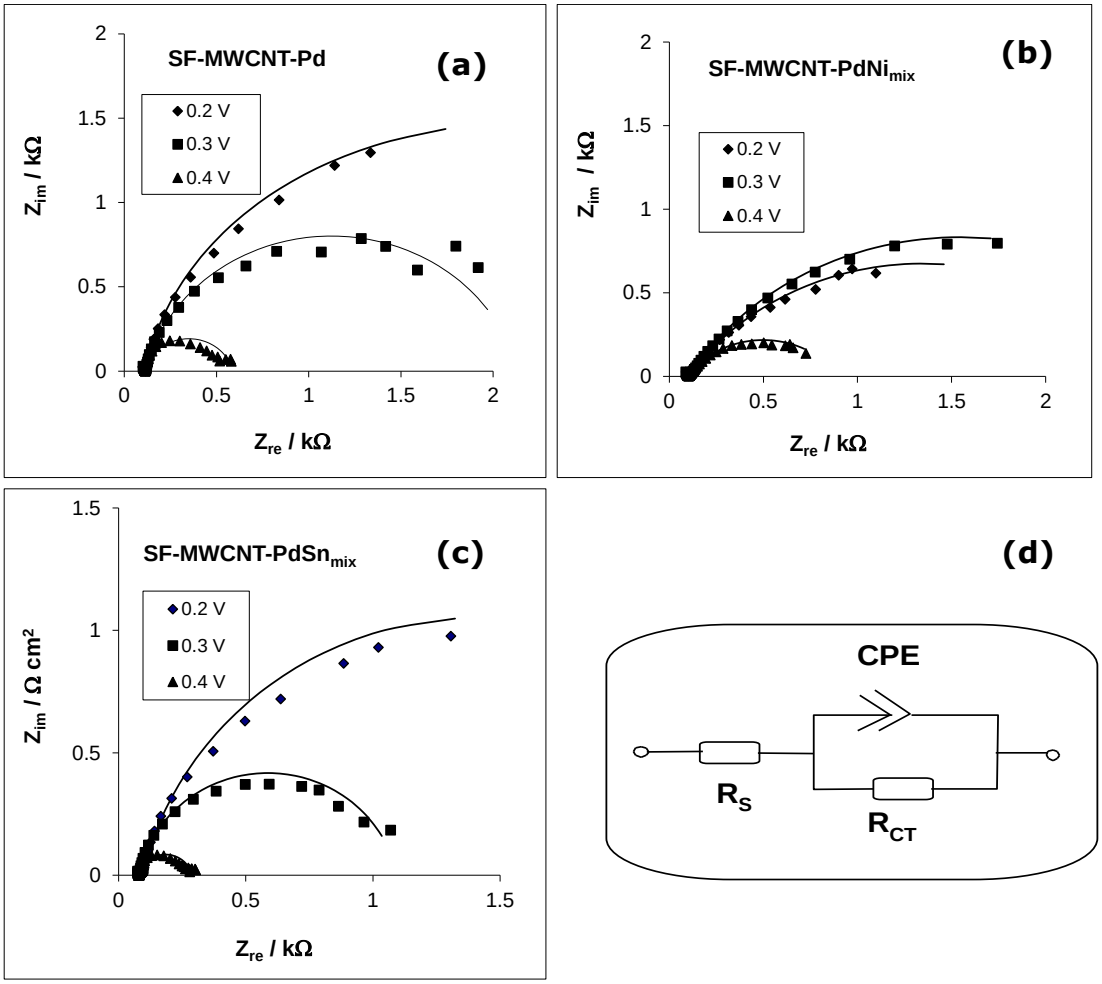

Figure 4: Nyquist plots obtained during the oxidation of ethylene glycol oxidation at (a) SF-MWCNT-Pd, (b) SF-MWCNT-PdNi$_{mix}$, and SF-MWWCNT-PdSn$_{mix}$ electrodes, and (d) is the equivalent circuit used in fitting the electrochemical impedance spectra.